IEM-FT-193/99
CERN-TH/99-142
hep-ph/9905381

Nearly degenerate neutrinos, Supersymmetry and radiative corrections

J.A. Casas[1,2*], **J.R. Espinosa**[2†‡], **A. Ibarra**[1§] and **I. Navarro**[1¶]

[1] Instituto de Estructura de la materia, CSIC
Serrano 123, 28006 Madrid
[2] Theory Division, CERN
CH-1211 Geneva 23, Switzerland.

Abstract

If neutrinos are to play a relevant cosmological rôle, they must be essentially degenerate with a mass matrix of the bimaximal mixing type. We study this scenario in the MSSM framework, finding that if neutrino masses are produced by a see-saw mechanism, the radiative corrections give rise to mass splittings and mixing angles that can accommodate the atmospheric and the (large angle MSW) solar neutrino oscillations. This provides a natural origin for the $\Delta m^2_{sol} \ll \Delta m^2_{atm}$ hierarchy. On the other hand, the vacuum oscillation solution to the solar neutrino problem is always excluded. We discuss also in the SUSY scenario other possible effects of radiative corrections involving the new neutrino Yukawa couplings, including implications for triviality limits on the Majorana mass, the infrared fixed point value of the top Yukawa coupling, and gauge coupling and bottom-tau unification.

CERN-TH/99-142
May 1999

*E-mail: casas@mail.cern.ch
†E-mail: espinosa@mail.cern.ch.
‡On leave of absence from Instituto de Matemática y Física Fundamental, CSIC, Madrid (Spain)
§E-mail: alejandro@makoki.iem.csic.es
¶Email: ignacio@makoki.iem.csic.es

1 Introduction

If neutrinos are to play a relevant cosmological role, their masses should be $\mathcal{O}$(eV). In that case, since atmospheric and solar neutrino anomalies [1] indicate that mass-squared splittings are at most 10^{-2} eV^2, neutrinos must be almost degenerate [2]-[5]. On the other hand, supersymmetry (SUSY) is a key ingredient in most of the extensions of the Standard Model (SM) which are candidate for a more fundamental theory. In this paper we will analyze, within the supersymmetric framework, under which circumstances the "observed" mass splittings between quasi-degenerate neutrinos arise naturally (or not), as a radiative effect, in agreement with all the available experimental data.

This problem has been also addressed in a recent paper by Ellis and Lola [6], in which they treat the neutrino mass matrix, $\mathcal{M}_\nu$, as an effective operator, emerging at some scale, Λ, with the bimaximal mixing form. Then the renormalization group (RG) analysis shows that the splittings and mixings at low energy are not in agreement with observations. Here we take a more general point of view. Besides exploring the effective operator scenario, we focus our attention in the (well motivated) case in which this operator is produced by a see-saw mechanism[2]. This introduces crucial differences in the analysis. In particular, the form of $\mathcal{M}_\nu$ is modified by a first stage of RG running of the neutrino Dirac-Yukawa matrix and the right-handed neutrino mass matrix from the high energy scale (say M_p or M_{GUT}) to Λ, which is identified with the Majorana mass scale. As we will see, this modification allows in many cases to reconcile the scenario with experiment, providing also a natural origin for the "observed" solar-atmospheric hierarchy of splittings, $\Delta m^2_{sol} \ll \Delta m^2_{at}$.

In a recent paper [9], we performed a similar analysis in the SM framework (in which the only particles added to the SM are three right-handed neutrinos), also with positive results. There are similarities and differences between the SUSY and the SM cases. First, SUSY introduces additional unknowns in the scenario, particularly the supersymmetric mass spectrum. In the analysis, the only rôle of this spectrum is to give the threshold scale(s) below which the effective theory is just the SM. In this sense, the combination of (negative) experimental data and naturalness requires $M_{SUSY} \sim 1$

[2]An alternative possibility to generate small non-zero neutrino masses in the MSSM involves R-parity breaking [7]. See Ref. [8] for a discussion on the interplay between the two possibilities.

TeV. Of course, there may be appreciable differences between the masses of various supersymmetric particles (squarks, gluino, charginos, etc.). Still, the variation in the results of the RG analysis are not important. Hence, we will take a unique threshold at $M_{SUSY} = 1$ TeV throughout the paper. Let us mention here that, apart from three right-handed neutrinos, we will assume a minimal spectrum of particles; in other words we will work within the minimal supersymmetric standard model (MSSM). Second (and more important), in the supersymmetric regime, the charged-lepton Yukawa couplings are multiplied by a factor $1/\cos\beta$ with respect to their SM value. These couplings (together with the neutrino Yukawa couplings) play a major rôle in the radiative modification of the form of $\mathcal{M}_\nu$. Thus, the results are going to present a strong dependence on $\tan\beta$ (we recall that $\tan\beta$ is defined as the ratio of the expectation values of the two supersymmetric Higgs doublets, $\tan\beta \equiv \langle H_2^0\rangle/\langle H_1^0\rangle$). Finally, the renormalization group equations (RGEs) themselves are different in the SUSY and in the SM cases. The difference is not just quantitative (i.e. differences in the size of the various coefficients), but also qualitative. In particular, the modification of the $\mathcal{M}_\nu$ texture due to the contribution from the charged-lepton Yukawa couplings has opposite signs in the two cases (while the contribution from the neutrino Yukawa couplings themselves remains with the same sign).

Let us briefly review the current relevant experimental constraints on neutrino masses and mixing angles (a more detailed account is given in ref. [9]). Observations of atmospheric neutrinos are well described by $\nu_\mu - \nu_\tau$ oscillations driven by a mass splitting and a mixing angle in the range [10]

$$\begin{aligned} 5\times 10^{-4}\ \mathrm{eV}^2 < \Delta m^2_{at} < 10^{-2}\ \mathrm{eV}^2\ , \\ \sin^2 2\theta_{at} \quad > \quad 0.82\ . \end{aligned} \tag{1}$$

Concerning the solar neutrino problem, as has been shown in ref. [2] the small angle MSW solution is unplausible in a scenario of nearly degenerate neutrinos, so we are left with the large angle MSW (LAMSW) and the vacuum oscillation (VO) solutions, which require mass splittings and mixing angles in the following ranges

LAMSW solution:

$$\begin{aligned} 10^{-5}\ \mathrm{eV}^2 < \ \Delta m^2_{sol}\ < 2\times 10^{-4}\ \mathrm{eV}^2, \\ 0.5 < \sin^2 2\theta_{sol} < 1. \end{aligned} \tag{2}$$

VO solution:

$$5 \times 10^{-11}\ \mathrm{eV}^2 < \Delta m^2_{sol} < 1.1 \times 10^{-10}\ \mathrm{eV}^2,$$
$$\sin^2 2\theta_{sol} \quad > \quad 0.67\,. \tag{3}$$

From the previous equations, it is apparent the hierarchy of mass splittings between the different species of neutrinos, $\Delta m^2_{sol} \ll \Delta m^2_{at}$, which should be reproduced by any natural explanation of those splittings. Let us also remark that it is not clear at the moment the value of the upper bound on $\sin^2 2\theta_{sol}$ [see eq.(2)]. As we will see, an upper limit like $\sin^2 2\theta_{sol} < 0.99$ or even greater, may disallow the scenario examined in this paper. For the moment, we will not consider any upper bound on $\sin^2 2\theta_{sol}$ (see ref.[9] for a more detailed discussion). On the other hand, according to the most recent combined analysis of SK + CHOOZ data (last paper of ref. [10]) the third independent angle, say ϕ (the one mixing the electron with the most split mass eigenstate), is constrained to have low values, $\sin^2 2\phi < 0.36\,(0.64)$ at 90% (99%) C.L.

Other relevant experimental information concerns the non-observation of neutrinoless double β-decay, which requires the ee element of the $\mathcal{M}_\nu$ matrix to be bounded as [11]

$$\mathcal{M}_{ee} < B = 0.2\ \mathrm{eV}. \tag{4}$$

In addition, Tritium β-decay experiments indicate $m_{\nu_i} < 2.5$ eV for any mass eigenstate with a significant ν_e component [12]. Finally, concerning the cosmological relevance of neutrinos, we will take $\sum m_{\nu_i} = 6$ eV as a typical possibility and we will explain how the results vary when this value is changed.

Let us introduce now some notation. In the SUSY framework the effective mass term for the three light (left-handed) neutrinos in the flavour basis is given by a term in the superpotential

$$W_{eff} = \frac{1}{2}\nu^T \mathcal{M}_\nu \nu\ . \tag{5}$$

The mass matrix, $\mathcal{M}_\nu$, is diagonalized in the usual way, i.e. $\mathcal{M}_\nu = V^* D\, V^\dagger$, where $D = \mathrm{diag}(m_1 e^{i\phi}, m_2 e^{i\phi'}, m_3)$ and V is a unitary 'CKM' matrix, relating flavour to mass eigenstates

$$\begin{pmatrix} \nu_e \\ \nu_\mu \\ \nu_\tau \end{pmatrix} = \begin{pmatrix} c_2 c_3 & c_2 s_3 & s_2 e^{-i\delta} \\ -c_1 s_3 - s_1 s_2 c_3 e^{i\delta} & c_1 c_3 - s_1 s_2 s_3 e^{i\delta} & s_1 c_2 \\ s_1 s_3 - c_1 s_2 c_3 e^{i\delta} & -s_1 c_3 - c_1 s_2 s_3 e^{i\delta} & c_1 c_2 \end{pmatrix} \begin{pmatrix} \nu_1 \\ \nu_2 \\ \nu_3 \end{pmatrix}\ . \tag{6}$$

Here s_i and c_i denote $\sin\theta_i$ and $\cos\theta_i$, respectively. In the following we will label the mass eigenvectors ν_i as $m^2_{\nu_1} < m^2_{\nu_2}$ and $|\Delta m^2_{12}| < |\Delta m^2_{23}|$, where $\Delta m^2_{ij} \equiv m^2_j - m^2_i$ ($m^2_{\nu_3}$ is thus the most split eigenvalue). In this notation, constraint (4) reads

$$\mathcal{M}_{ee} \equiv |m_{\nu_1}\, c_2^2 c_3^2 e^{i\phi} + m_{\nu_2}\, c_2^2 s_3^2 e^{i\phi'} + m_{\nu_3}\, s_2^2\, e^{i2\delta}| < B\,. \tag{7}$$

As it has been put forward by Georgi and Glashow in ref. [2], a scenario of nearly degenerate neutrinos should be close to a bimaximal mixing, which constrains the texture of the mass matrix $\mathcal{M}_\nu$ to be essentially [2,3]

$$\mathcal{M}_b = m_\nu \begin{pmatrix} 0 & \frac{1}{\sqrt{2}} & \frac{1}{\sqrt{2}} \\ \frac{1}{\sqrt{2}} & \frac{1}{2} & -\frac{1}{2} \\ \frac{1}{\sqrt{2}} & -\frac{1}{2} & \frac{1}{2} \end{pmatrix}\,, \tag{8}$$

where m_ν gives an overall mass scale. $\mathcal{M}_b$ can be diagonalized by a V matrix

$$V_b = \begin{pmatrix} \frac{-1}{\sqrt{2}} & \frac{1}{\sqrt{2}} & 0 \\ \frac{1}{2} & \frac{1}{2} & \frac{-1}{\sqrt{2}} \\ \frac{1}{2} & \frac{1}{2} & \frac{1}{\sqrt{2}} \end{pmatrix}\,, \tag{9}$$

leading to exactly degenerate neutrinos, $D = m_\nu\ \mathrm{diag}(-1,1,1)$, and $\theta_2 = 0$, $\sin^2 2\theta_3 = \sin^2 2\theta_1 = 1$.

It is quite conceivable that $\mathcal{M}_\nu = \mathcal{M}_b$ could be generated at some high scale by interactions obeying appropriate continuous or discrete symmetries [13]. However, in order to be realistic, $\mathcal{M}_\nu$ at low energy should be *slightly* different from $\mathcal{M}_b$ to account for the mass splittings given in eqs.(1–3). We will explore whether the appropriate splittings (and mixing angles) can be generated or not through radiative corrections; more precisely, through the running of the RGEs from the high scale down to low energy. As discussed in ref.[9], the output of this analysis can be of three types:

i) All the mass splittings and mixing angles obtained from the RG running are in agreement with all experimental limits and constraints.

ii) Some (or all) mass splittings are much larger than the acceptable ranges.

iii) Some (or all) mass splittings are smaller than the acceptable ranges, and the rest is within.

Case *(i)* is fine, while case *(ii)* is disastrous. Case *(iii)* is not fine, but it admits the possibility that other (not specified) effects could be responsible for the splittings. Concerning the mixing angles, it has been stressed in refs. [6,9] that due to the two degenerate eigenvalues of $\mathcal{M}_b$, V_b is not uniquely defined. Hence, once the ambiguity is removed thanks to the small splittings coming from the RG running, the mixing angles may be very different from the desired ones. If such cases correspond to the previous *(iii)* possibility, they could still be rescued since the modifications on $\mathcal{M}_\nu$ (of non-specified origin) needed to reproduce the correct mass splittings will also change dramatically the mixing angles.

In section 2, we examine the general case in which the neutrino masses arise from an effective operator, remnant from new physics entering at a scale Λ. In this framework, we assume a bimaximal-mixing mass structure at the scale Λ as an initial condition and do not consider possible perturbations of that initial condition coming from the new physics entering at Λ. If $\tan\beta$ is small the LAMSW scenario in this case is of the undecidable type [possibility *(iii)* above], but for $\tan\beta$ above a certain value which we compute, it is excluded (the VO solution is excluded for any $\tan\beta$).

In section 3 we consider in detail a particularly well motivated example for the new physics beyond the scale Λ introduced before: the see-saw scenario. We include here the high energy effects of the new degrees of freedom above the scale Λ (identified now with the mass scale of the right-handed neutrinos). We find regions of parameter space where the neutrino spectrum and mixing angles fall naturally in the pattern required to explain solar (LAMSW solution) and atmospheric neutrino anomalies, which we find remarkable. We complement the numerical results, presented in section 4, with compact analytical formulas which give a good description of them, and allow to understand the pattern of mass splittings and mixing angles obtained. We also present plausible textures for the neutrino Yukawa couplings leading to a good fit of the oscillation data.

Section 5, still in the see-saw framework, discusses several possible implications of the effect of large neutrino couplings on: triviality limits on the Majorana mass; the infrared fixed point value of the top Yukawa coupling, with consequences for the lower limit on $\tan\beta$ and the value of the Higgs mass; and gauge coupling and bottom-tau unification. Finally we draw some conclusions.

2 $\mathcal{M}_\nu$ as an effective operator

In this section we will simply assume that the effective mass matrix for the left-handed neutrinos, $\mathcal{M}_\nu$, is generated at some high energy scale, Λ, by some unspecified mechanism. Assuming that below Λ the effective theory is the MSSM with unbroken $R-$parity, the lowest dimension operator in the superpotential producing a mass of this kind is [14]

$$W_{eff} = \frac{1}{4}\kappa\nu^T\nu H_2^0 H_2^0 \,, \tag{10}$$

where κ is a matricial coupling and H_2^0 is the neutral component of the $Y = +1/2$ Higgs field (the one coupled to the $u-$quarks). Obviously, $\mathcal{M}_\nu = \frac{1}{2}\kappa\langle H_2^0\rangle^2$. Between Λ and M_{SUSY}, the effective coupling κ runs with the scale with a RGE [14]

$$16\pi^2\frac{d\kappa}{dt} = \kappa\left[-\frac{6}{5}g_1^2 - 6g_2^2 + 6Y_t^2\right] + \left[\kappa\mathbf{Y_e^\dagger Y_e} + (\mathbf{Y_e^\dagger Y_e})^T\kappa\right] \,, \tag{11}$$

where $t = \log\mu$, and $g_2, g_1, Y_t, \mathbf{Y_e}$ are the $SU(2)\times U(1)_Y$ gauge couplings, the (MSSM) top Yukawa coupling and the (MSSM) matrix of Yukawa couplings for the charged leptons respectively. Between M_{SUSY} and M_Z κ runs with the SM RGE [14]

$$16\pi^2\frac{d\kappa}{dt} = \left[-3g_2^2 + 2\lambda + 6\tilde{Y_t}^2 + 2\mathrm{Tr}\tilde{\mathbf{Y}}_\mathbf{e}^\dagger\tilde{\mathbf{Y}}_\mathbf{e}\right]\kappa - \frac{1}{2}\left[\kappa\tilde{\mathbf{Y}}_\mathbf{e}^\dagger\tilde{\mathbf{Y}}_\mathbf{e} + (\tilde{\mathbf{Y}}_\mathbf{e}^\dagger\tilde{\mathbf{Y}}_\mathbf{e})^T\kappa\right] \,, \tag{12}$$

where λ is the SM quartic Higgs coupling and $\tilde{Y_t}$, $\tilde{\mathbf{Y}}_\mathbf{e}$ correspond to the SM Yukawa couplings [the matching at M_{SUSY} is $\tilde{Y_t}(M_{SUSY}) = \sin\beta\, Y_t(M_{SUSY})$, $\tilde{\mathbf{Y}}_\mathbf{e}(M_{SUSY}) = \cos\beta\,\mathbf{Y_e}(M_{SUSY})$].

In a scenario of almost degenerate neutrinos, the simplest assumption for the initial form of the matricial coupling, $\kappa(\Lambda)$ is just the bimaximal mixing texture of eq.(8), and this was also the assumption made in refs.[6,9]. In consequence,

$$\mathcal{M}_\nu(\Lambda) = \frac{1}{2}\kappa(\Lambda)\langle H_2^0\rangle^2 = \frac{1}{2}\kappa(\Lambda)\sin^2\beta v^2 = \mathcal{M}_b \,, \tag{13}$$

where $v^2 = \langle H_1^0\rangle^2 + \langle H_2^0\rangle^2 = (175\,\mathrm{GeV})^2$. The last terms in eqs.(11, 12), i.e. those depending on $\mathbf{Y_e^\dagger Y_e}$, are generation-dependent and will modify the $\mathcal{M}_\nu$ texture, thus generating mass splittings and changing the mixing angles. It is easy to see [6,9] that, in first approximation, the splittings $\Delta m_{ij}^2 \equiv m_j^2 - m_i^2$ have the form

$$\Delta m_{12}^2 \;=\; -\frac{1}{2}\Delta m_{13}^2 \;=\; -\frac{1}{3}\Delta m_{23}^2 \;\simeq\; -m_\nu^2\epsilon > 0. \tag{14}$$

where, neglecting for a while all the charged lepton Yukawa couplings but Y_τ, and working in the approximation of constant RGE β functions, ϵ is given by

$$\epsilon = \frac{\tilde{Y_\tau}^2}{32\pi^2}\left[-\frac{2}{\cos^2\beta}\log\frac{\Lambda}{M_{SUSY}} + \log\frac{M_{SUSY}}{\mu_0}\right]. \tag{15}$$

Thus, the SUSY and the SM corrections have opposite signs. If $(\Lambda/M_{SUSY})^{2/\cos^2\beta} > M_{SUSY}/\mu_0$, as it is the usual case, ϵ has negative sign and the most split eigenvalue is the smallest one [thus the convention of labels used in eq.(14)]. Notice also that the pure SM case is recovered setting $M_{SUSY} = \Lambda$. As in the SM case, the previous spectrum is not realistic, i.e. the splittings are barely able to reproduce simultaneously the Δm^2_{sol} and Δm^2_{at} splittings given in eqs.(1–3). Actually, the size of the splittings is larger than in the pure SM case (due to the coefficients of the RGEs and, especially, to the dependence on $\cos\beta$). This makes the scenario potentially more difficult than the SM one (see the discussion in the Introduction).

Fig.1 shows the complete numerical evaluation of the RGEs for $m_\nu = 2$ eV and $\tan\beta = 2$, which corroborates the structure of eqs.(14, 15). The splittings are always much larger than those required for the VO solution to the solar neutrino problem, $\Delta m^2_{sol} \sim 10^{-10}$ eV^2. Therefore, the effect of the RGEs for this scenario is disastrous in the sense discussed in the Introduction for the possibility *(ii)*. In consequence, as for the pure SM case, the VO solution to the solar neutrino problem is excluded[3]. For the LAMSW solution to the solar neutrino problem, things are a bit different. The smallest mass splitting is always within (or not far larger than) the LAMSW range, which indicates that we are in the situation (*iii*) explained in the Introduction (not satisfactory, but it may be rescued by extra physics). When m_ν is varied the results change with the scaling law $\Delta m^2_{ij} \propto m^2_\nu$.

The dependence of the splittings on $\tan\beta$ is quite strong. Fig.2 shows this dependence for $\Lambda = 10^{10}$ GeV. Even for moderate values of $\tan\beta$ the smallest splitting is much larger than the LAMSW range, thus spoiling that solution. Therefore, for a given value of Λ and m_ν, the viability of the supersymmetric scenario of nearly degenerate neutrinos puts an upper bound on $\tan\beta$. A reasonable estimate for this upper bound is given in Fig.3, which shows the value of $\tan\beta$ (vs. Λ) for which the small-

[3]Notice from the figure and from eq.(15) that there is a value of Λ (close to M_{SUSY}) for which the splittings vanish, but of course the fine-tuning required for Λ to be close enough to that point, so that the splittings are within the VO range, is enormous.

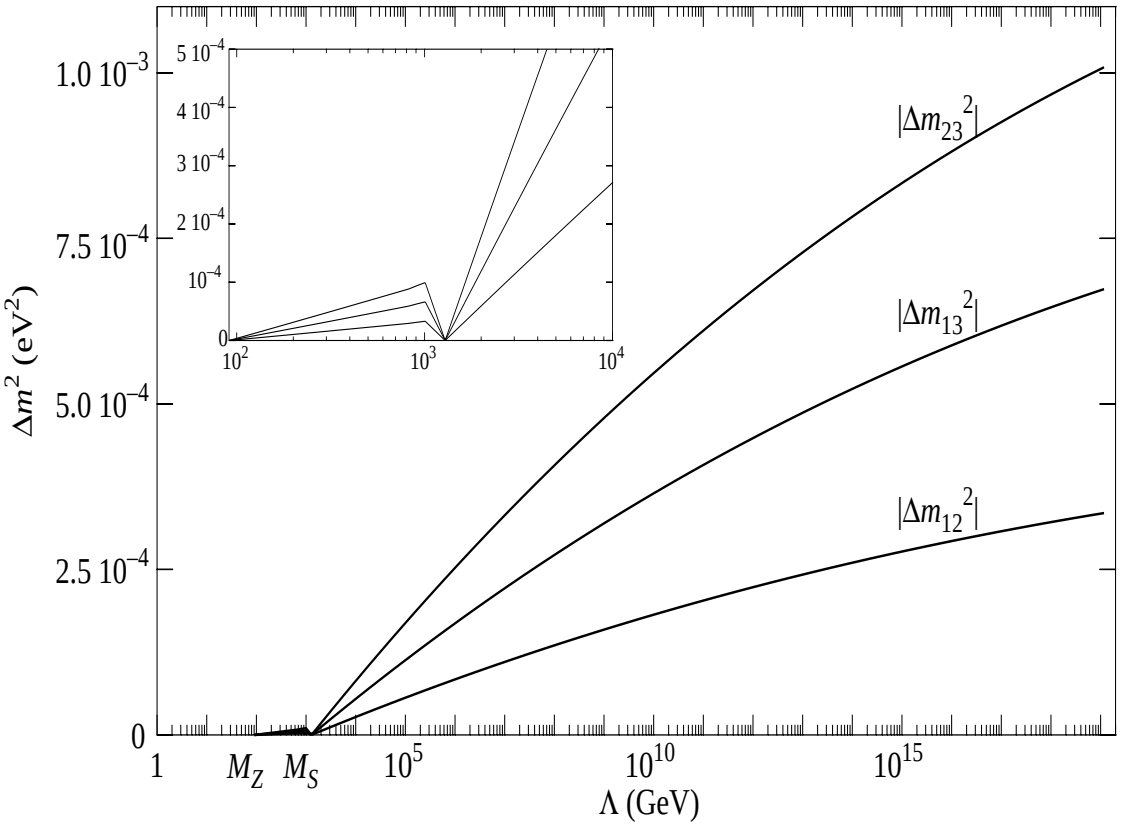

Figure 1: Dependence of neutrino mass splittings at low energy (Δm^2_{ij} in eV^2) with the cut-off scale Λ(GeV). For this figure $\tan\beta = 2$.

est splitting generated is larger (and ten times larger), than the maximum acceptable LAMSW value. The upper curve is therefore a conservative bound. These bounds become weaker if the neutrino mass, m_ν, decreases, as it follows from the previously mentioned scaling law.

Concerning the mixing angles, in a first approximation the 'CKM' matrix, V, is given by

$$V \simeq \begin{pmatrix} -\frac{1}{\sqrt{2}} & \frac{1}{\sqrt{3}} & \frac{1}{\sqrt{6}} \\ \frac{1}{2} & \sqrt{\frac{2}{3}} & -\frac{1}{2\sqrt{3}} \\ \frac{1}{2} & 0 & \frac{\sqrt{3}}{2} \end{pmatrix}, \tag{16}$$

which leads to mixing angles

$$\sin^2 2\theta_1 = \frac{9}{25}, \quad \sin^2 2\theta_2 = \frac{5}{9}, \quad \sin^2 2\theta_3 = \frac{24}{25}. \tag{17}$$

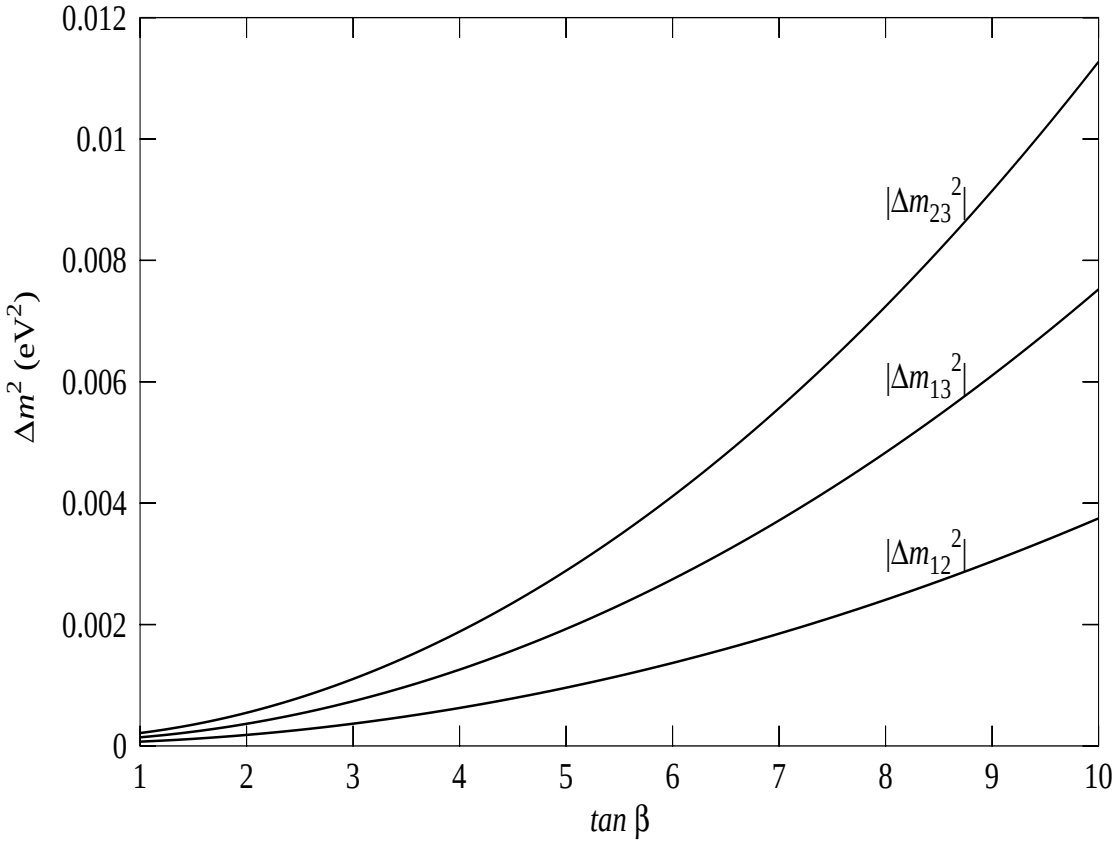

Figure 2: Dependence of neutrino mass splittings at low energy (Δm^2_{ij} in eV^2) with $\tan\beta$, for $\Lambda = 10^{10}$GeV.

These values are far away from the bimaximal mixing ones. In consequence, they are not acceptable, stressing the fact that the simplified scenario discussed in this section does not work. However, as explained in the Introduction, if extra effects are able to modify the form of $\mathcal{M}_\nu$ in order to produce the correct splittings, this modification will also change drastically the mixing angles, hopefully in a positive direction. This leads us to the see-saw scenario, which is analyzed in the next section.

3 $\mathcal{M}_\nu$ from the see-saw mechanism

The simplest example of the kind of new physics appearing at a scale Λ which can generate an effective mass term for the low-energy neutrinos we observe is the so-called see-saw mechanism [15]. Its supersymmetric version has superpotential

$$W = W_{MSSM} - \frac{1}{2}\nu^c_R \mathcal{M} \nu^c_R + \nu^c_R \mathbf{Y}_\nu L \cdot H_2, \tag{18}$$

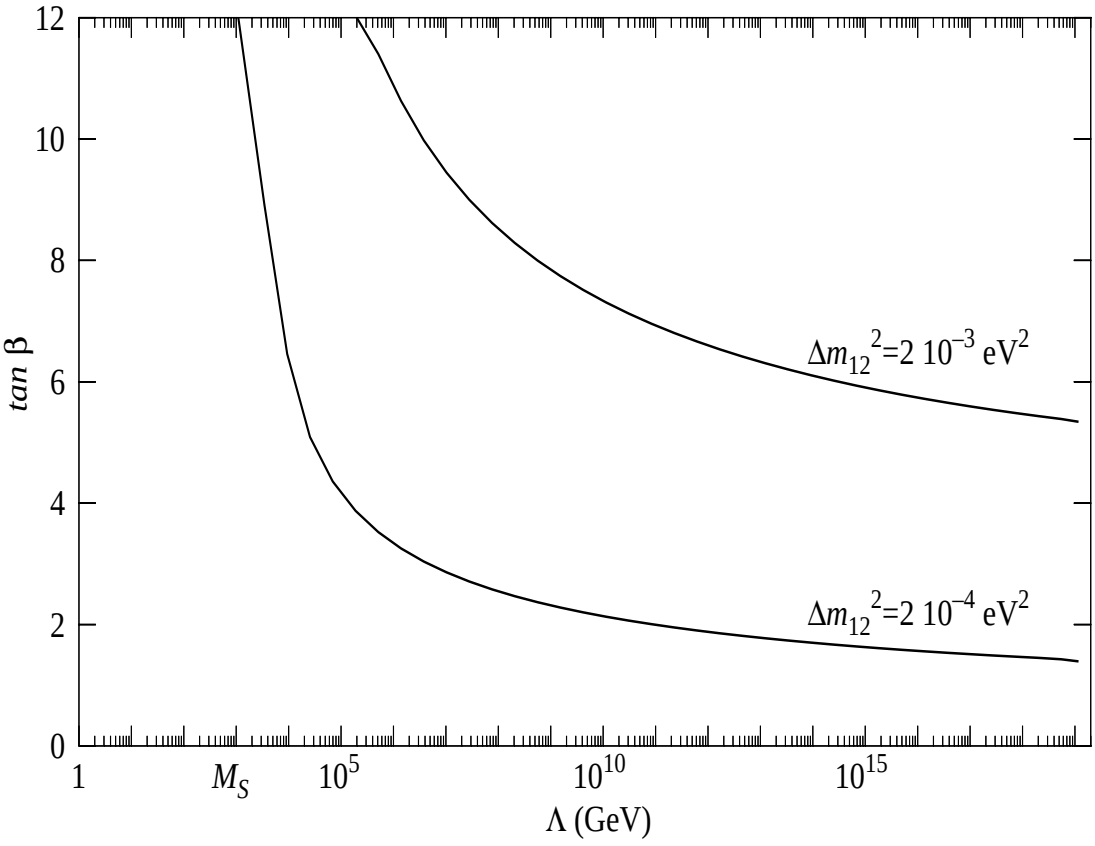

Figure 3: Upper limit on $\tan\beta$, as a function of Λ, beyond which the smallest neutrino mass splitting is larger (lower curve), or ten times larger (upper curve), than the maximum acceptable LAMSW value.

where W_{MSSM} is the superpotential of the MSSM. The extra terms involve three additional neutrino chiral fields (one per generation; indices are suppressed) not charged under the SM group: $\nu_{\alpha,R}$ ($\alpha = e, \mu, \tau$). $\mathbf{Y}_\nu$ is the matrix of neutrino Yukawa couplings and H_2 is the hypercharge $+1/2$ Higgs doublet. Now, the Dirac mass matrix is $\mathbf{m_D} = \mathbf{Y}_\nu v \sin\beta$. Finally, $\mathcal{M}$ is a 3×3 Majorana mass matrix which does not break the SM gauge symmetry. It is natural to assume that the overall scale of $\mathcal{M}$, which we will denote by M, is much larger than the electroweak scale or any soft mass. Below M the theory is governed by an effective superpotential

$$W_{eff} = W_{MSSM} + \frac{1}{2}(\mathbf{Y}_\nu L \cdot H_2)^T \mathcal{M}^{-1} (\mathbf{Y}_\nu L \cdot H_2), \tag{19}$$

obtained by integrating out the heavy neutrino fields in (18). From this effective superpotential, the Lagrangian contains a mass term for the left-handed neutrinos:

$$\delta\mathcal{L} = -\frac{1}{2}\nu^T \mathcal{M}_\nu \nu + \text{h.c.}, \tag{20}$$

with

$$\mathcal{M}_\nu = \mathbf{m_D}^T \mathcal{M}^{-1} \mathbf{m_D} = \mathbf{Y}_\nu{}^T \mathcal{M}^{-1} \mathbf{Y}_\nu \langle H_2^0 \rangle^2, \tag{21}$$

suppressed with respect to the typical fermion masses by the inverse power of the large scale M.

The approximate degeneracy of neutrino masses in this framework follows from the initial condition for the neutrino mass matrix at the Planck scale: $\mathcal{M}_\nu(M_p) = \mathcal{M}_b$, which would lead to exactly degenerate neutrino masses. We do not address in this paper the possible origin of this very symmetric form. As explained in [9], to explore the simplest (and most natural) textures of $\mathbf{Y}_\nu$ and $\mathcal{M}$ leading to this initial condition it is enough to consider the case in which the Majorana mass matrix is

$$\mathcal{M} = M \begin{pmatrix} -1 & 0 & 0 \\ 0 & 1 & 0 \\ 0 & 0 & 1 \end{pmatrix}, \tag{22}$$

and all the structure is in the Yukawa matrix, which reads

$$\mathbf{Y}_\nu = Y_\nu B V_b^T . \tag{23}$$

Here Y_ν is the overall magnitude of $\mathbf{Y}_\nu$ and B is a combination of two 'boosts'

$$B = \begin{pmatrix} \cosh a & 0 & \sinh a \\ 0 & 1 & 0 \\ \sinh a & 0 & \cosh a \end{pmatrix} \begin{pmatrix} \cosh b & \sinh b & 0 \\ \sinh b & \cosh b & 0 \\ 0 & 0 & 1 \end{pmatrix}, \tag{24}$$

with two free parameters a, b. Having all the structure in the Majorana matrix and $\mathbf{Y}_\nu \propto \mathbf{I_3}$ is equivalent to the case $a = b = 0$. We will present our results, for fixed values of M and $\tan\beta$, in the (a, b) plane demanding $|a|, |b| \leq 1.5$. If $|a|$ or $|b|$ are larger than 1.5 the matrix elements of $\mathbf{Y}_\nu$ are fine-tuned at least in a 10% [9].

The neutrino masses, exactly degenerate at tree-level by assumption, will receive generation dependent radiative corrections which will lift that degeneracy, eventually reproducing the pattern of mass splittings necessary to interpret the experimental indications. The bulk of these radiative corrections is logarithmic and easy to compute by standard renormalization group techniques: one starts at M_p with (22) and (23) as boundary conditions and integrates down in energy the relevant RGEs in a supersymmetric theory which is the MSSM with three right-handed neutrino chiral fields and the superpotential (18). At the scale M the $\nu_{R,\alpha}$ are decoupled and below this scale

the running is performed exactly as in the previous section, except that now we have precise boundary conditions for the couplings and masses at M.

From M_p to M the evolution of the relevant matrices is governed by the following renormalization group equations [16]:

$$\frac{d\mathbf{Y}_\nu}{dt} = -\frac{1}{16\pi^2}\mathbf{Y}_\nu\left[\left(3g_2^2+\frac{3}{5}g_1^2-\mathrm{T}_2\right)\mathbf{I_3}-\left(3\mathbf{Y}_\nu{}^\dagger\mathbf{Y}_\nu+\mathbf{Y_e}^\dagger\mathbf{Y_e}\right)\right], \tag{25}$$

$$\frac{d\mathbf{Y_e}}{dt} = -\frac{1}{16\pi^2}\mathbf{Y_e}\left[\left(3g_2^2+\frac{9}{5}g_1^2-\mathrm{T}_1\right)\mathbf{I_3}-\left(\mathbf{Y}_\nu{}^\dagger\mathbf{Y}_\nu+3\mathbf{Y_e}^\dagger\mathbf{Y_e}\right)\right], \tag{26}$$

where

$$\mathrm{T}_1 = \mathrm{Tr}(3\mathbf{Y_D}^\dagger\mathbf{Y_D}+\mathbf{Y_e}^\dagger\mathbf{Y_e}), \quad \mathrm{T}_2 = \mathrm{Tr}(3\mathbf{Y_U}^\dagger\mathbf{Y_U}+\mathbf{Y}_\nu^\dagger\mathbf{Y}_\nu), \tag{27}$$

and

$$\frac{d\mathcal{M}}{dt} = \frac{1}{8\pi^2}\left[\mathcal{M}(\mathbf{Y}_\nu\mathbf{Y}_\nu{}^\dagger)^T+\mathbf{Y}_\nu\mathbf{Y}_\nu{}^\dagger\mathcal{M}\right], \tag{28}$$

(not yet given in the literature). Here g_2 and g_1 are the $SU(2)_L$ and $U(1)_Y$ gauge coupling constants, and $\mathbf{Y_{U,D,e}}$ are the Yukawa matrices for up quarks, down quarks and charged leptons.

At M, ν_R decouple, and $\mathbf{Y_e}$ must be diagonalized to redefine the flavour basis of leptons [note that the last term in (26) produces non-diagonal contributions to $\mathbf{Y_e}$] affecting the form of the $\mathbf{Y}_\nu$ matrix. Then the effective mass matrix for the light neutrinos is $\mathcal{M}_\nu \simeq \mathbf{Y}_\nu{}^T\mathcal{M}^{-1}\mathbf{Y}_\nu\langle H_2^0\rangle^2$.

From M to M_Z, the effective mass matrix $\mathcal{M}_\nu$ is run down in energy exactly as described in section 2.

The renormalization group equations are integrated with the following boundary conditions: $\mathcal{M}$ and $\mathbf{Y}_\nu$ are chosen at M_p so as to satisfy

$$\mathcal{M}_\nu(M_p) = \mathcal{M}_b, \tag{29}$$

with the overall magnitude of $\mathbf{Y}_\nu$ fixed, for a given value of the Majorana mass M, by the requirement $m_\nu \sim \mathcal{O}(\mathrm{eV})$. We will take $m_\nu = 2$ eV as a guiding example. The boundary conditions for the other Yukawa couplings are also fixed at the low energy side to give the observed fermion masses. The free parameters are therefore $M, \tan\beta, a$ and b.

3.1 Analytical integration of the RGEs

It is simple and very illuminating to integrate analytically the renormalization group equations (11,25,26,28) in the approximation of constant right hand side. In this approximation (which works very well for our analysis), the effective neutrino mass matrix at low-energy is simply $\mathcal{M}_b$ plus some small perturbation. The overall mass scale is fixed to be of order 2 eV, so we need only to pay attention to the non-universal terms in the RGEs, which will be responsible for the mass splittings. Neglecting the Y_e, Y_μ Yukawa couplings, we get the following analytical expressions (the labelling of mass eigenvalues below may not always correspond to the conventional order $m^2_{\nu_1} < m^2_{\nu_2}$, $|\Delta m^2_{12}| < |\Delta m^2_{23}|$):

$$\begin{aligned} m_{\nu_1} &\simeq m_\nu \left[-1 + (2c_a^2 c_b^2 - 1)\epsilon_\nu - 2\epsilon_\tau\right], \\ m_{\nu_{2,3}} &\simeq m_\nu \left[1 + 3\epsilon_\tau - c_a^2 c_b^2 \epsilon_\nu \pm \left\{\left[\epsilon_\tau + (c_a^2 c_b^2 - c_{2a})\epsilon_\nu\right]^2 + \left[s_{2a} s_b \epsilon_\nu - 2\sqrt{2}\epsilon_\tau\right]^2\right\}^{1/2}\right] \end{aligned} \tag{30}$$

where $c_a = \cosh a$, $s_{2a} = \sinh 2a$, etc. These expressions are identical to the ones derived in [9] for the SM case, except for the numerical values of ϵ_τ and ϵ_ν, which are now given by:

$$\epsilon_\tau = \frac{Y_\tau^2}{128\pi^2}\left[-2\log\frac{M_p}{M_{SUSY}} + \cos^2\beta \log\frac{M_{SUSY}}{M_Z}\right], \tag{31}$$

$$\epsilon_\nu = \frac{Y_\nu^2}{8\pi^2}\log\frac{M_p}{M}. \tag{32}$$

The Yukawa couplings in these expressions should be chosen at an appropriate intermediate scale but the simple formulas (31,32) are good enough for our purpose. Note also that Y_ν and Y_τ have an implicit dependence on $\tan\beta$ and, furthermore Y_ν depends strongly on M (due to the requirement $m_\nu \sim 2$ eV).

There are important differences with respect to the SM case presented in [9]: 1) ϵ_τ is insensitive to the Majorana threshold, its sign is negative (it was positive in the SM) and it grows in magnitude for increasing $\tan\beta$; 2) ϵ_ν is twice larger than in the SM and decreases slightly when $\tan\beta$ increases.

In the case $a = b = 0$, the mass splittings are independent of ϵ_ν and similar to those found in section 2, that is, not satisfactory (remember that this case is equivalent to having all the structure in $\mathcal{M}$, while $\mathbf{Y}_\nu$ is proportional to the identity and thus universal).

For a given M, there is a critical value of $\tan\beta$ below (above) which $|\epsilon_\tau|$ is smaller (larger) than ϵ_ν. This critical value of $\tan\beta$ increases with M. When $\epsilon_\nu \gg |\epsilon_\tau|$, we can further expand the neutrino masses in powers of $\epsilon_\tau/\epsilon_\nu$ finding

$$\begin{aligned} m_{\nu_1} &\simeq m_\nu \left[-1 + (2c_a^2 c_b^2 - 1)\epsilon_\nu - 2\epsilon_\tau\right], \\ m_{\nu_2} &\simeq m_\nu \left[1 - (2c_a^2 c_b^2 - 1)\epsilon_\nu + \left(2 - \frac{1 - c_{2a} - 2\sqrt{2}s_{2a}s_b}{c_a^2 c_b^2 - 1}\right)\epsilon_\tau\right], \\ m_{\nu_3} &\simeq m_\nu \left[1 - \epsilon_\nu + \left(4 + \frac{1 - c_{2a} - 2\sqrt{2}s_{2a}s_b}{c_a^2 c_b^2 - 1}\right)\epsilon_\tau\right]. \end{aligned} \tag{33}$$

Here we clearly see that the small mass splitting (solar) is controlled by the small parameter ϵ_τ, proportional to the squared Yukawa couplings of the charged leptons, while ϵ_ν (proportional to the square of the larger Yukawa coupling Y_ν) is responsible for the larger mass difference (atmospheric). Moreover, the two neutrino eigenstates closest in mass (m_{ν_1}, m_{ν_2}) have masses of opposite sign, which is exactly what is required to fulfill the neutrinoless double β-decay condition, eq.(7). In the SM case, for values of M between 10^9 and 10^{12} GeV, ϵ_τ and ϵ_ν have the right orders of magnitude to account for Δm^2_{sol}, Δm^2_{at} [9]. In the supersymmetric scenario it is still the case that ϵ_ν gives the correct atmospheric mass splitting, but for $m_\nu = 2$ eV ϵ_τ gives typically a Δm^2_{sol} one order of magnitude too high (recall here that by lowering m_ν this splitting becomes smaller following the approximate law $\Delta m^2 \propto m_\nu^2$). This means that in this case only in particular regions of the (a, b) plane, in which some mild cancellation is taking place, we will obtain the right mass splitting to solve the solar neutrino problem. This cancellation does occur in regions around the lines $a = 0$ and $2\sqrt{2}\sinh b = -\tanh a$ for which, in the approximation (33), $m^2_{\nu_1} = m^2_{\nu_2}$. In those regions then, we have a natural explanation for the Δm^2_{sol} mass splitting while Δm^2_{at} requires only a mild fine-tuning of parameters.

If $\epsilon_\nu \ll |\epsilon_\tau|$, then a different expansion shows that there is no natural hierarchy of mass splittings, which tend to be of the same order. In these cases, a stronger fine-tuning is required to get small enough Δm^2_{sol} and the regions in parameter space where this occurs shrink, again around $1 - c_{2a} - 2\sqrt{2}s_{2a}s_b = 0$. However, Δm^2_{at} is still naturally of the right order of magnitude.

Turning to the mixing angles, it is easy to see that the eigenvectors of the perturbed

$\mathcal{M}_\nu$ matrix are of the form

$$V_1' = V_1, \quad V_2' = \frac{1}{\sqrt{\alpha^2+\beta^2}}(\alpha V_2 + \beta V_3), \quad V_3' = \frac{1}{\sqrt{\alpha^2+\beta^2}}(-\beta V_2 + \alpha V_3), \qquad (34)$$

where V_i are the eigenstates corresponding to the bimaximal mixing matrix, V_b [see eq.(9)]

$$V_1 = \begin{pmatrix} \frac{-1}{\sqrt{2}} \\ \frac{1}{2} \\ \frac{1}{2} \end{pmatrix}, \quad V_2 = \begin{pmatrix} \frac{1}{\sqrt{2}} \\ \frac{1}{2} \\ \frac{1}{2} \end{pmatrix}, \quad V_3 = \begin{pmatrix} 0 \\ \frac{-1}{\sqrt{2}} \\ \frac{1}{\sqrt{2}} \end{pmatrix}. \qquad (35)$$

In the approximation $|\epsilon_\tau| \ll \epsilon_\nu$, the parameters α, β are given by

$$\alpha = c_a s_b + \mathcal{O}(\epsilon_\tau/\epsilon_\nu), \quad \beta = s_a + \mathcal{O}(\epsilon_\tau/\epsilon_\nu). \qquad (36)$$

The V_i' vectors define the new 'CKM' matrix V' from which the mixing angles are extracted. In the case of interest, the spectrum of neutrinos consists of two lightest states ($m_{\nu_{1,2}}$) very close in mass and a heavier one m_{ν_3}. The relative ordering in mass of $m_{\nu_{1,2}}$ is not fixed and this affects the relative order of V_1' and V_2' in the V' matrix. This has an effect on the sign of $\cos 2\theta_3$, which is important for the MSW condition $\cos 2\theta_3 > 0$ (written using the conventional order $m^2_{\nu_1} < m^2_{\nu_2}$). This will be satisfied as long as V_1 corresponds to the lightest mass eigenvalue. In other words, this condition requires that the negative mass eigenvalue, see eqs.(30, 33), corresponds to the lightest neutrino. On the other hand, the relative ordering of the two lightest neutrinos does not change the values of $\sin^2 2\theta_i$.

In this approximation, if just one of the two (a, b) parameters is vanishing, then $V' = V_b$, i.e. exactly the bimaximal mixing case. Also, whenever c_a, c_b are sizeable (i.e. away from $a = b = 0$), $|\alpha| \gg |\beta|$, and thus we are close to the bimaximal case. Therefore, it is not surprising that in most of the parameter space this will be in fact the case. This is remarkable, because it gives a natural origin for the bimaximal mixing, which was not guaranteed a priori due to the ambiguity in the diagonalization of the initial $\mathcal{M}_\nu(M_p) = \mathcal{M}_b$ matrix, as was explained in the Introduction.

The only free parameter in the V' matrix is the ratio α/β and one obtains the relations:

$$\sin^2 2\theta_1 = \frac{(2r-1)^2}{(2r+1)^2}, \quad \sin^2 2\theta_2 = 1 - \frac{r^2}{(1+r)^2}, \quad \sin^2 2\theta_3 = 1 - \frac{1}{(1+2r)^2}, \qquad (37)$$

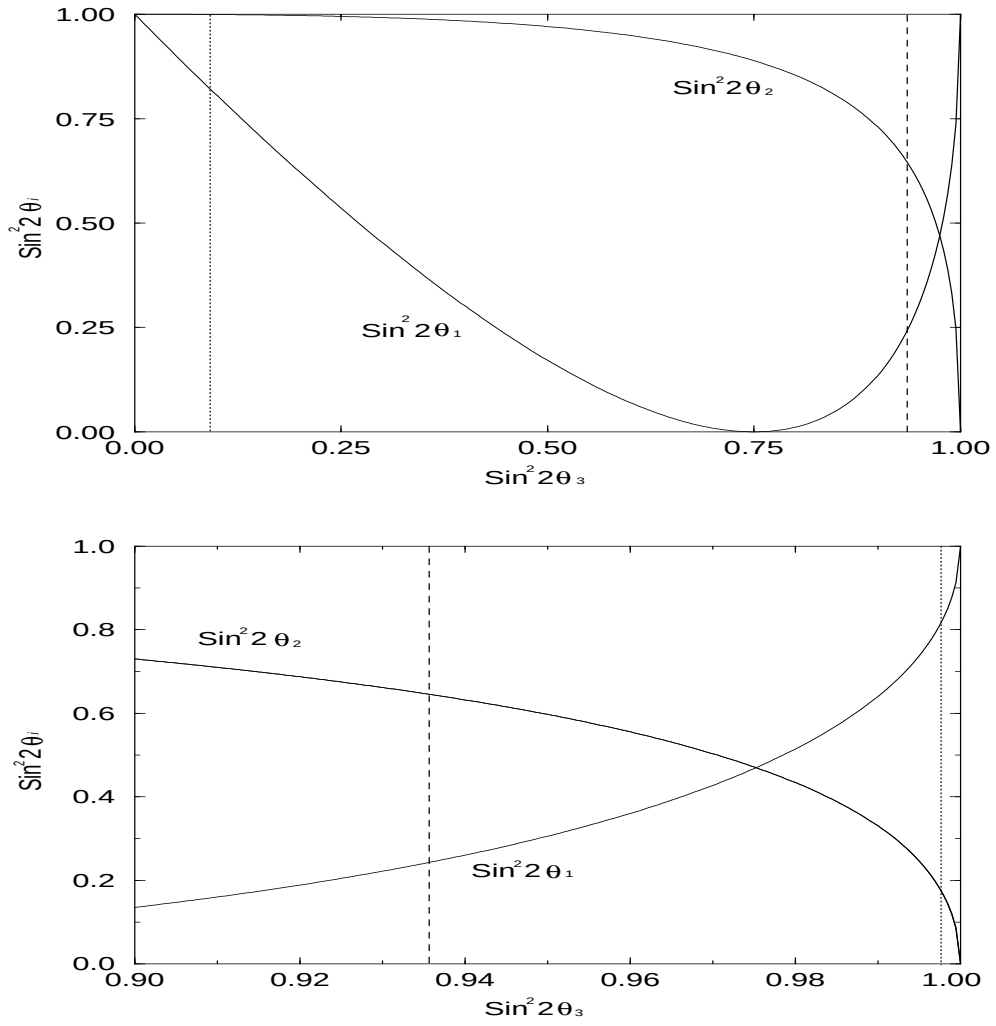

Figure 4: Upper plot: Neutrino mixing angles, $\sin^2 2\theta_1$ and $\sin^2 2\theta_2$, vs. $\sin^2 2\theta_3$ in the near degenerate scenario. Lower plot: Zoom of the $0.9 \leq \sin^2 2\theta_3 \leq 1$ region.

where $r \equiv \alpha^2/\beta^2$. It is instructive to invert the last relation, find r in terms of $\sin^2 2\theta_3$, and then substitute back in the two previous relations.

Figures 4a,b present $\sin^2 2\theta_{1,2}$ as functions of $\sin^2 2\theta_3$ obtained in this way. For clarity, figure 4b focuses on the region of $\sin^2 2\theta_3$ close to 1, which is the interesting one. We can impose the experimental limits on these angles directly in this figure. We see that the limit $\sin^2 2\theta_2 < 0.64$ (dashed line) translates into a lower limit $\sin^2 2\theta_3 \gtrsim 0.94$ (the region to the left of the dashed line is forbidden). In a similar way, $\sin^2 2\theta_1 > 0.82$ (dotted lines) requires either $\sin^2 2\theta_3 < 0.09$ (but this solution gives $\sin^2 2\theta_2 > 0.64$ and is not acceptable) or $\sin^2 2\theta_3 \gtrsim 0.9978$ (the region to the right of the dotted line in figure 4b is allowed). Note that if we impose the stringent condition $\sin^2 2\theta_3 < 0.99$, derived

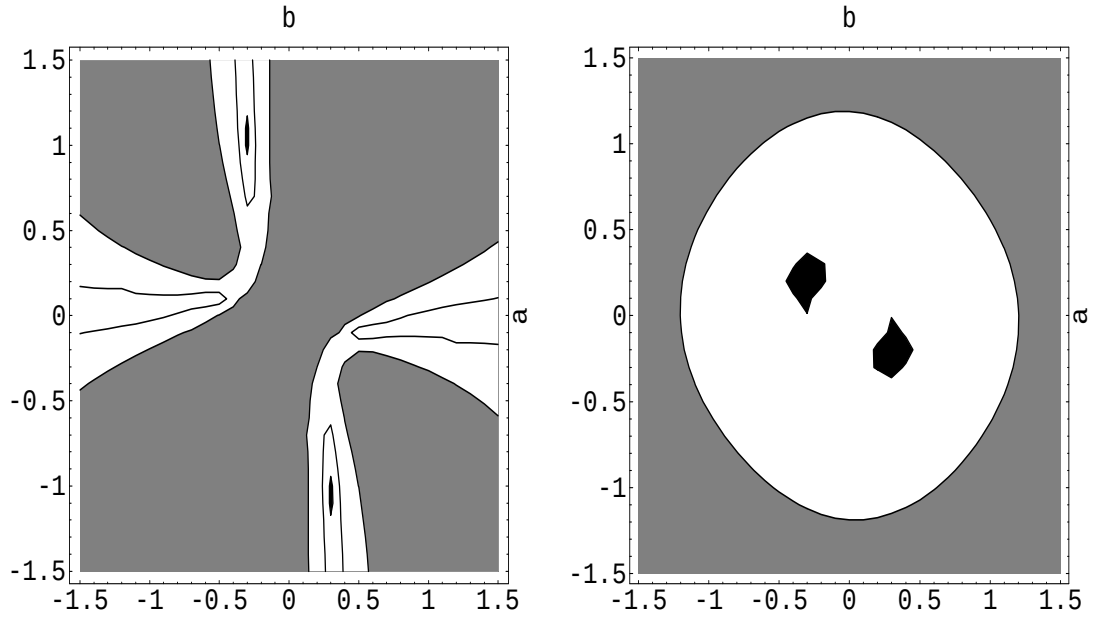

Figure 5: Left plot: contours of $\Delta m^2_{12}/\mathrm{eV}^2$ in the (b, a) plane from less than 10^{-5} (black area), through 6×10^{-5} (lines) to more than 2×10^{-4} (grey). Right plot: same for $\Delta m^2_{23}/\mathrm{eV}^2$, from 5×10^{-4} (black) to 10^{-2} (grey). The Majorana mass is 10^{10} GeV and $\tan\beta = 2$.

from some fits to solar data as discussed in the Introduction, then no viable solution would exist. Without such condition we find that this framework can accomodate the angles required by the data with

$$\sin^2 2\theta_1 \geq 0.82, \quad \sin^2 2\theta_2 \leq 0.17, \quad \sin^2 2\theta_3 \geq 0.9978. \tag{38}$$

Since, in first approximation, the perturbed $\mathcal{M}_\nu$ will have eigenvectors of the form (34), this result and the previous discussion are also valid for the SM case [9] and any model starting with $\mathcal{M}_\nu = \mathcal{M}_b$. Actually, the results shown in eq.(37) and Fig. 4 may be considered as predictions of such a kind of scenarios.

In the next section we show that there are regions in parameter space where both the mass splittings and the mixing angles have the right values to explain the solar and atmospheric neutrino data.

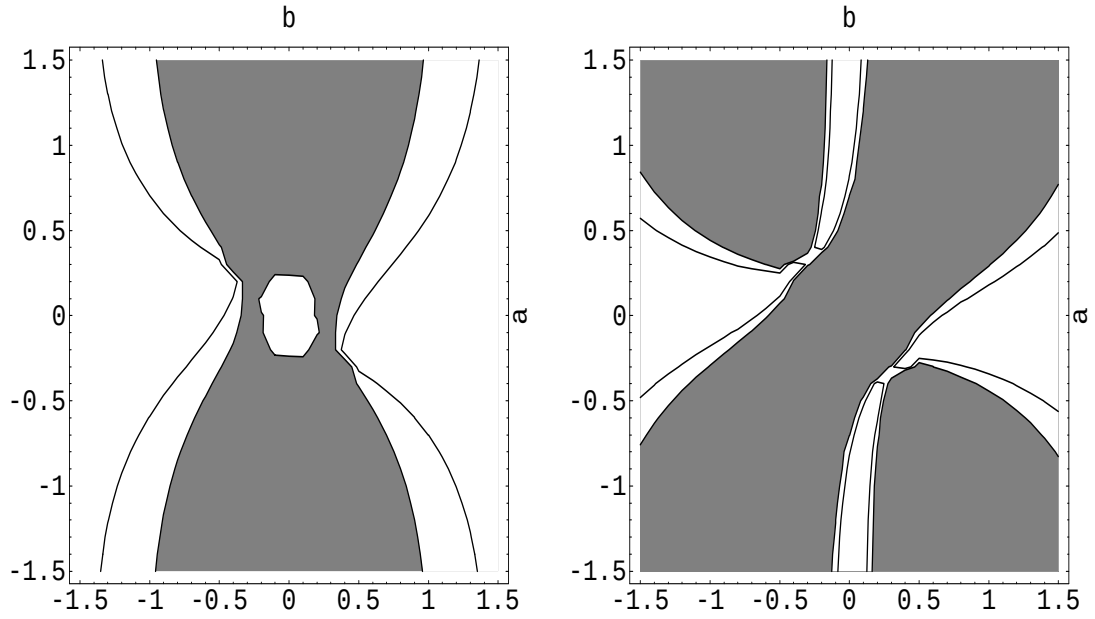

Figure 6: Left plot: Contours of $\sin^2 2\theta_2$ in the (b, a) plane. The grey area marks the $\sin^2 2\theta_2 > 0.64$ region. The line singled-out corresponds to $\sin^2 2\theta_2 = 0.36$. Right plot: Contours of $\sin^2 2\theta_1$ in the (b, a) plane. In the grey area $\sin^2 2\theta_1$ is smaller than 0.82, and the line corresponds to $\sin^2 2\theta_1 = 0.9$. The Majorana mass is 10^{10} GeV and $\tan\beta = 2$.

3.2 Numerical Results

Figures 5 to 10 present our results for the mass splittings and mixing angles at low energy, after numerical integration of the RGEs from M_p to M_Z as described in the previous sections. We stress that our convention in all the figures is to assign the indices 1 and 2 to the neutrino states closest in mass, with $m^2_{\nu_1} < m^2_{\nu_2}$ and leave the index 3 for the other neutrino state. In the interesting regions, where the parameters would fit well the solar and atmospheric data, the third neutrino is the heaviest. Hence, the neutrino spectrum has the same structure as in the SM case [9].

We start with the results for $M = 10^{10}$ GeV and $\tan\beta = 2$ chosen as a typical example; the dependence of the results with M and $\tan\beta$ is discussed afterwards. Figure 5, left plot, shows contour lines of constant Δm^2_{12} (the squared mass difference between the lightest neutrinos) in the plane (b, a). The black (grey) region is excluded because there $\Delta m^2_{12} < 10^{-5}\,\mathrm{eV}^2$ ($\Delta m^2_{12} > 2 \times 10^{-4}\,\mathrm{eV}^2$), which is too small (large) to account for the oscillations of solar neutrinos (LAMSW solution). The white area is

thus the allowed region. The line in it corresponds to $\Delta m^2_{12} = 6 \times 10^{-5}\,\mathrm{eV}^2$. Note how the allowed area is not too large and extends around the parametric line $1 - c_{2a} - 2\sqrt{2} s_{2a} s_b = 0$, as explained in the previous section.

Figure 5, right plot, gives contour lines of constant Δm^2_{23}. The black (grey) region is excluded because there $\Delta m^2_{23} < 5 \times 10^{-4}\,\mathrm{eV}^2$ ($\Delta m^2_{23} > 10^{-2}\,\mathrm{eV}^2$), which is too small (large) to account for the oscillations of atmospheric neutrinos. Again, the white area is allowed. The small black areas correspond in fact to the "undecidable" case discussed in the Introduction: they might be rescued by unspecified extra effects. We do not present a plot for Δm^2_{13} because it can always be inferred from Δm^2_{23} and Δm^2_{12}. Moreover, in the interesting case, $\Delta m^2_{12} \ll \Delta m^2_{23}$, one has $\Delta m^2_{13} \simeq \Delta m^2_{23}$.

The intersection of the white areas in both plots is non-zero and would give the allowed area concerning mass splittings. It is always the case that the area surrounding the origin is excluded. There, the mass differences are always of the same order, and follow the same pattern discussed in section 2 ($\Delta m^2_{23} = 2\Delta m^2_{12}$). In any case we conclude that, away from the origin, there is a non-zero region of parameter space where $\Delta m^2_{23} \gg \Delta m^2_{12}$, in accordance with the values required to explain the solar and atmospheric neutrino anomalies simultaneously.

For mixing angles, figure 6, left plot, gives contours of constant $\sin^2 2\theta_2$ (one of the mixing angles relevant for atmospheric neutrino oscillations). The grey (white) area has $\sin^2 2\theta_2$ larger (smaller) than 0.64 and is disfavored (favored) by the data (SK + CHOOZ) at 99% C.L. according to the most recent analysis (last paper of ref. [10]). The line singled-out corresponds to $\sin^2 2\theta_2 = 0.36$ (maximum allowed value at 90% C.L. according to the same reference). Figure 6, right plot, shows contours of constant $\sin^2 2\theta_1$ (the other mixing angle relevant for atmospheric neutrinos). The grey (white) area corresponds to $\sin^2 2\theta_1$ smaller (larger) than 0.82, and is thus disallowed (allowed). The additional line included has $\sin^2 2\theta_1 = 0.9$.

Finally, figure 7, left plot, presents contours of constant $\sin^2 2\theta_3$ which is relevant for oscillations of solar neutrinos. The grey (white) region has $\sin^2 2\theta_3$ larger (smaller) than 0.99. If one is willing to interpret the existing data as implying an upper bound of 0.99 on $\sin^2 2\theta_3$, then the grey region would be excluded. The plotted curves give $\sin^2 2\theta_3 = 0.95$. Figure 7, right plot, shows the region of the parameter space accomplishing the resonance condition ($\cos 2\theta_3 > 0$), which is required for an efficient MSW solution of the solar anomaly (see however the first paper of ref. [10] for caveats on this issue).

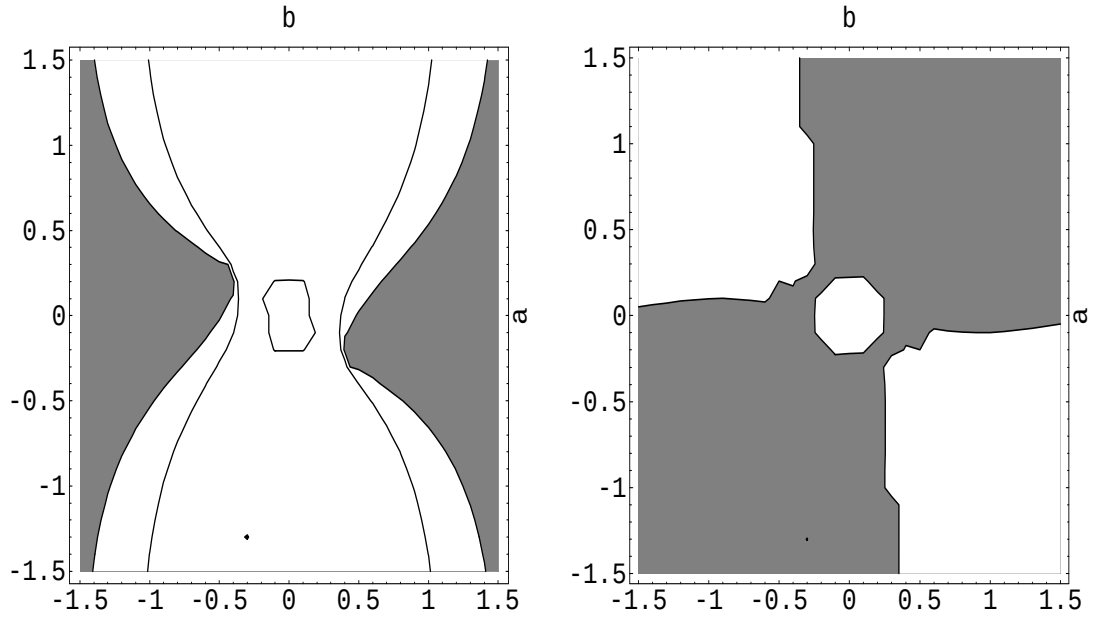

Figure 7: Left plot: Same as figure 6 for $\sin^2 2\theta_3$. The grey area corresponds to values above 0.99. The curves give $\sin^2 2\theta_3 = 0.95$. Right plot: The grey area corresponds to $\cos 2\theta_3 < 0$

The region of parameter space where all constraints on mixing angles and mass splittings are satisfied is given by the intersection of all white areas in figures 5, 6 and 7 (right plot). If $\sin^2 2\theta_3 < 0.99$ is imposed, then that intersection region, including now figure 7 (left plot), is empty and no allowed region remains. It should be noticed that this fact does not come from an incompatibility between the previous constraint and the $\sin^2 2\theta_3 > 0.99$ obtained from neutrinoless double β-decay limits, eq. (7), in the $\theta_2 = 0$ approximation. If this were the case, it could be easily solved by decreasing the overall size of the neutrino masses, m_ν, in eq.(7), and this is not the case. Indeed, eq.(7) is satisfied in nearly all the parameter space. Even where $\sin^2 2\theta_3 < 0.99$, this is still true thanks to the contribution of θ_2. What actually forbids the whole parameter space if $\sin^2 2\theta_3 < 0.99$ is imposed is the incompatibility between acceptable θ_1, θ_2 and θ_3 angles to fit simultaneously all the neutrino oscillation data, as can be seen from the figures and in agreement with the discussion of the previous subsection, see eq.(38). This fact remains when m_ν is decreased. In fact, the effect of decreasing m_ν is essentially an amplification of the figures shown here, which comes from the fact that for a given Majorana mass, the neutrino Yukawa couplings become smaller (the effect

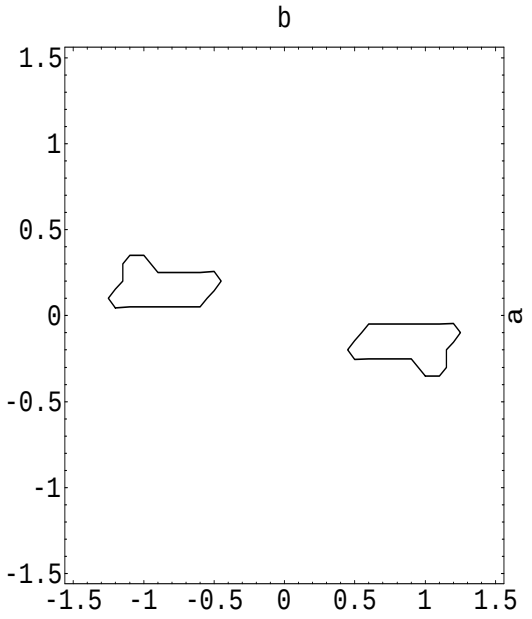

Figure 8: Region (two disconnected parts) in the (b, a) parameter space for $M = 10^{10}$ GeV and $\tan\beta = 2$ where all mass splittings and mixing angles satisfy experimental constraints. (See text for qualifications).

is similar to decreasing M, which is discussed below).

If the $\sin^2 2\theta_3 < 0.99$ condition is relaxed (as discussed in the Introduction), then the allowed region is given by the two islands in figure 8, which is non-negligible. It is remarkable that the small regions where all the mass splittings are of the right size and the small regions where the mixing angles are the appropriate ones have a non-zero overlapping.

The dependence of the results with the Majorana mass M is illustrated by figure 9, where the allowed regions in the plane (b, a) are shown for two different Majorana masses, $M = 10^9$ and 10^{11} GeV, keeping $\tan\beta = 2$. For comparison with the allowed region for $M = 10^{10}$ GeV (given in figure 8) we see that for small M the allowed region grows and flies away from the origin, until it leaves the naturalness region $|a|, |b| < 1.5$. For $M = 10^8$ GeV no allowed region inside the natural range for (a, b) remains. Conversely, increasing M reduces the allowed region, which gets closer to the origin (at $M = 10^{12}$ GeV the allowed region becomes extinct).

Concerning the remaining parameter, $\tan\beta$, figure 10 gives the allowed regions for

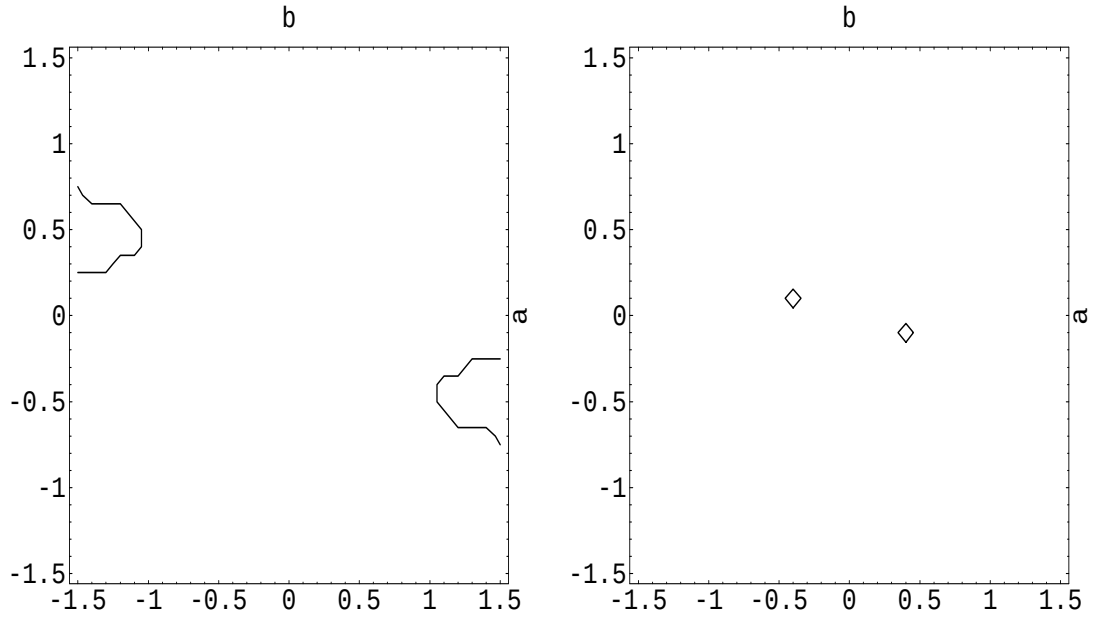

Figure 9:
Same as figure 8 for $\tan\beta = 2$ and different values of the Majorana mass. Left plot: $M = 10^9$ GeV; Right plot: 10^{11} GeV.

$M = 10^{10}$ GeV and four different values of $\tan\beta$: 1.75, 3, 4 and 6.5, as indicated. The minimum in $\tan\beta$ is dictated by the requirement of perturbativity of all couplings up to the Planck scale, banning the presence of a Landau pole below it, as discussed in section 5. The allowed region gets smaller and smaller when $\tan\beta$ increases. As explained in the previous section, $|\epsilon_\tau|$ grows with $\tan\beta$ making harder and harder a cancellation that gives the correct Δm^2_{sol} and mixing angles. Eventually, for $\tan\beta \gtrsim 6.5$ the allowed region disappears (for $M = 10^{11}$ GeV that value is $\tan\beta \gtrsim 3.5$).

Finally, let us stress that, if the $\sin^2 2\theta_3 < 0.99$ condition is imposed, the whole parameter space becomes disallowed for any value of M and $\tan\beta$. We also find that, whenever there is a hierarchy in the mass splittings, the two lightest eigenvalues have opposite signs. This is just what is needed to have a cancellation occurring in the neutrinoless double β-decay constraint (7). This constraint is satisfied in almost the whole parameter space for any M.

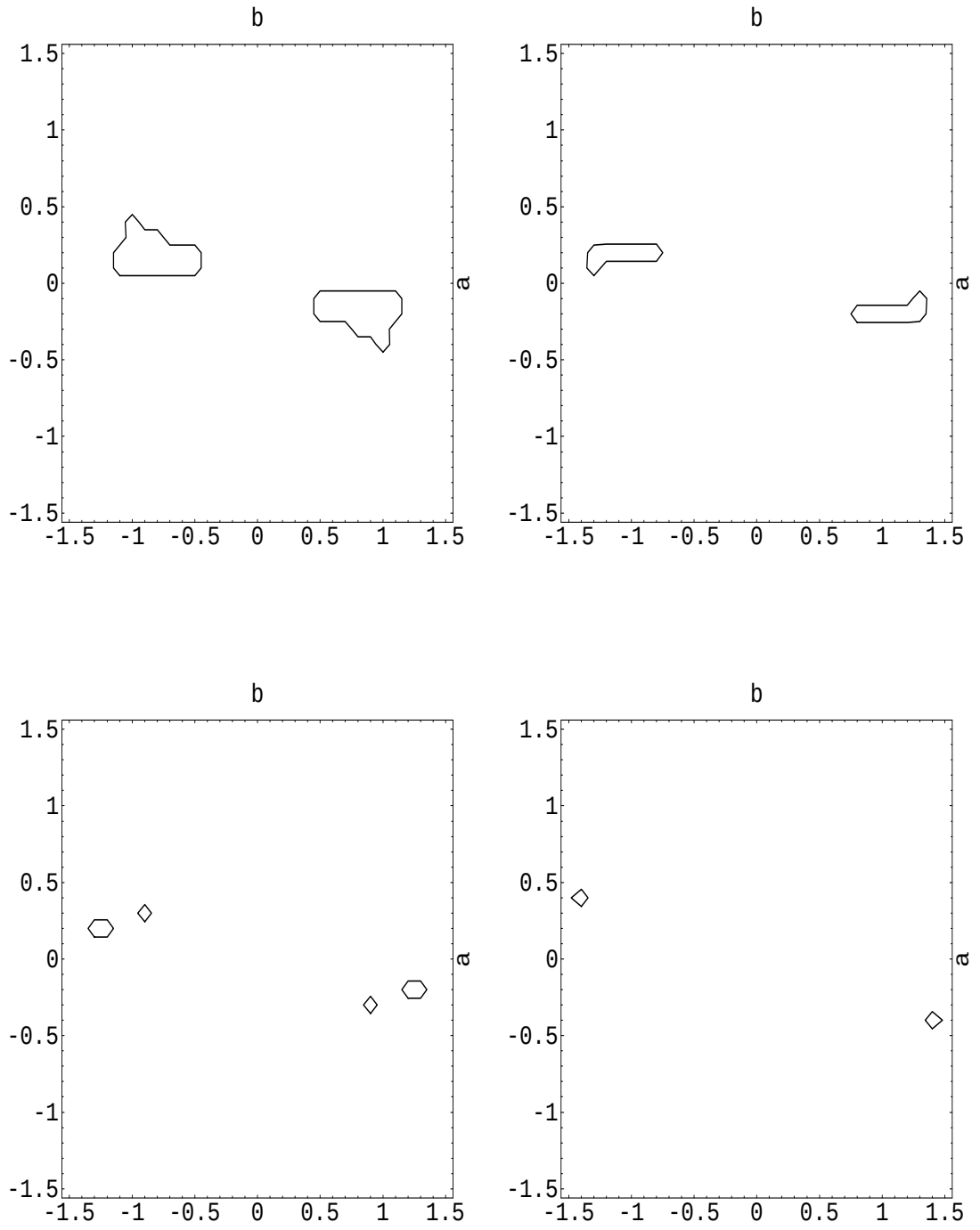

Figure 10:
Same as figure 8 for $M = 10^{10}$ GeV and different values of $\tan\beta$. Upper left: $\tan\beta = 1.75$. Upper right: 3. Lower left: 4. Lower right: 6.5.

4 Examples of acceptable ansätze

It is possible to find examples of matrices $\mathbf{Y}_\nu(M_p)$ which both fall inside the allowed areas presented in the previous section and are natural (perhaps pointing to a possible underlying symmetry).

An example, already presented in [9], which still survives in the supersymmetric case (for $M \sim 10^{10}\,\mathrm{GeV}$ and $\tan\beta \sim 2$) is

$$\mathbf{Y}_\nu(M_p) = Y_\nu \begin{pmatrix} -\dfrac{1}{2\sqrt{2}} & 1 & 1 \\ \dfrac{1}{2\sqrt{2}} & 1 & 1 \\ 0 & -\dfrac{1}{\sqrt{2}} & \dfrac{1}{\sqrt{2}} \end{pmatrix}. \tag{39}$$

It corresponds to $a = 0$ and $b = \sinh^{-1}(3/4) \simeq 0.69$. The mass splittings are

$$\Delta m^2_{12} \simeq 1 \times 10^{-4}\,\mathrm{eV}^2, \quad \Delta m^2_{13} \simeq 2 \times 10^{-3}\,\mathrm{eV}^2, \quad \Delta m^2_{23} \simeq 2 \times 10^{-3}\,\mathrm{eV}^2, \tag{40}$$

and the mixing angles

$$\sin^2 2\theta_2 = 0.082, \quad \sin^2 2\theta_1 = 0.9163, \quad \sin^2 2\theta_3 = 0.99954, \tag{41}$$

with $\cos 2\theta_3$ at the border of the resonance condition for the MSW mechanism.

Another examples of working ansätze can be obtained. For instance, the following ansatz (corresponding to $a = -\cosh^{-1}(\sqrt{5}/2) \simeq -0.48$, $b = \log(\sqrt{10}/2) \simeq 1.15$)

$$\mathbf{Y}_\nu(M_p) = Y_\nu \begin{pmatrix} -\dfrac{1}{4} & \dfrac{3}{\sqrt{2}} & \sqrt{2} \\ \dfrac{1}{2\sqrt{5}} & \dfrac{\sqrt{5}}{2} & \dfrac{\sqrt{5}}{2} \\ \dfrac{1}{4\sqrt{5}} & -\dfrac{\sqrt{5}}{2} & 0 \end{pmatrix}, \tag{42}$$

works correctly for $M \sim 10^9$ GeV and $\tan\beta \sim 2$, giving

$$\Delta m^2_{12} \simeq 1 \times 10^{-4}\,\mathrm{eV}^2, \quad \Delta m^2_{13} \simeq 9 \times 10^{-4}\,\mathrm{eV}^2, \quad \Delta m^2_{23} \simeq 8 \times 10^{-4}\,\mathrm{eV}^2, \tag{43}$$

and the mixing angles

$$\sin^2 2\theta_2 = 0.02, \quad \sin^2 2\theta_1 = 0.979, \quad \sin^2 2\theta_3 = 0.99997, \tag{44}$$

with $\cos 2\theta_3 > 0$. It could be interesting to explore possible symmetries that may be responsible for the form of these ansätze and to analyze their implications for future long-baseline experiments [18].

5 Other relevant implications of neutrino-induced radiative corrections

The previous sections focussed on the possibility of reproducing the "observed" neutrino mass splittings from supersymmetric radiative corrections. In particular we analyzed the case of nearly degenerate neutrinos, which is closely related to the bimaximal mixing scenario.

In this section, still working in a see-saw framework, we take a different point of view and analyze the physical impact of neutrino-induced radiative corrections. The results of this section are quite generic. They are not associated to the bimaximal mixing scenario, not even to a scenario of degenerate neutrinos, but we will take this case as a representative example to illustrate the phenomena. Some of the following effects have already been mentioned along the paper, but here they are studied in greater detail.

The first topic concerns the appearance of Landau poles associated to the neutrinos and the corresponding implications. It is easy to check from eq.(25) that the neutrino Yukawa couplings, $\mathbf{Y}_\nu$, have a supersymmetric RGE quite similar to the top Yukawa coupling. It is therefore not surprising that they can develop Landau poles at high energy in a similar way. Obviously, the larger the right-handed neutrino Majorana mass, M, and the larger the low energy neutrino masses, m_ν, the larger the neutrino Yukawa couplings, thus lowering the scale at which the Landau pole appears. Consequently, if, in order to preserve perturbation theory (and the nice supersymmetric gauge coupling unification), we demand that the Landau pole does not appear below M_p (or the preferred high-energy scale), this puts upper bounds on M and m_ν (see ref.[17] for the analogue in the SM framework).

To analyze this effect, we will use the simplest textures of $\mathbf{Y}_\nu$ and $\mathcal{M}$, leading to a bimaximal mass matrix, namely $\mathbf{Y}_\nu = Y_\nu \mathbf{I_3}$ and $\mathcal{M}(M_p) \propto \mathcal{M}_b$ [$\mathcal{M}$ has exactly the form given in eq.(8) but with overall scale M instead of m_ν]. Recall that this is equivalent to the case $a = b = 0$ in the analysis of textures performed in section 3. Obviously, for $a, b \neq 0$ the neutrino Yukawa couplings are larger and the corresponding bounds stronger. Hence, we are analyzing here the most conservative case

To extract the bounds, we set the Landau pole of Y_ν at M_p (i.e. $Y_\nu(M_p) \gg 1$) and evaluate the corresponding low energy value of m_ν, through the renormalization

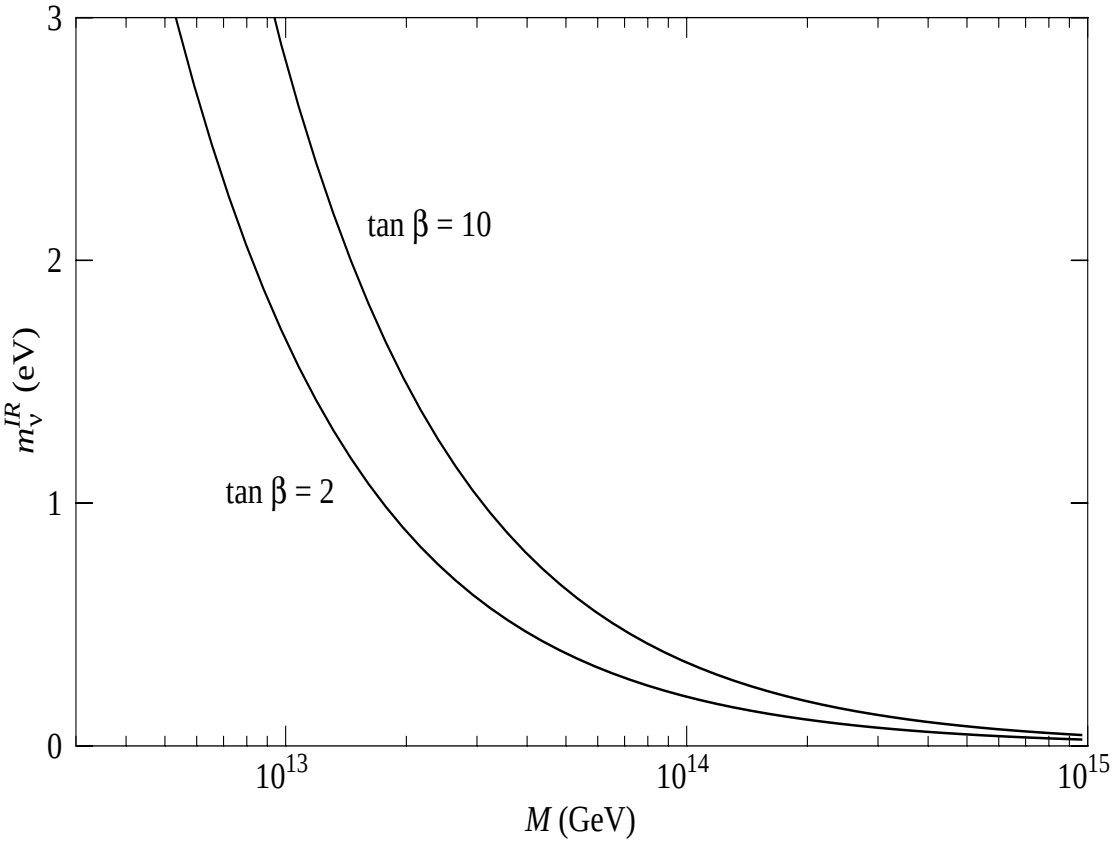

Figure 11: Upper bound on the neutrino mass, m_ν^{IR}, vs. the Majorana mass M for two different values of $\tan\beta$.

group equations of Y_ν (between M_p and M) and κ (below M), for a certain value of the Majorana mass M. This "infrared fixed point" value, say m_ν^{IR}, represents an upper bound for the neutrino mass. The dependence of m_ν^{IR} on M is illustrated in Fig. 11 for two different values of $\tan\beta$ (the value of M in the plot is to be understood as evaluated at the $M-$scale itself). Alternatively, for a particular value of the neutrino mass, m_ν, we can extract from the figure the upper bound on the Majorana mass. We note that the bounds are quite strong. For quite moderate values of the neutrino masses, they conflict with the possibility of a Majorana mass of $\mathcal{O}(M_{GUT})$.

A different issue concerns the appearance of limits on $\tan\beta$. In section 2, it was shown that the scenario of nearly degenerate neutrinos is in conflict with large values of $\tan\beta$, the reason being that the radiative corrections to the mass splittings become much larger than the observed ones. The bounds were shown in Fig.3, for $m_\nu = 2$ eV. For

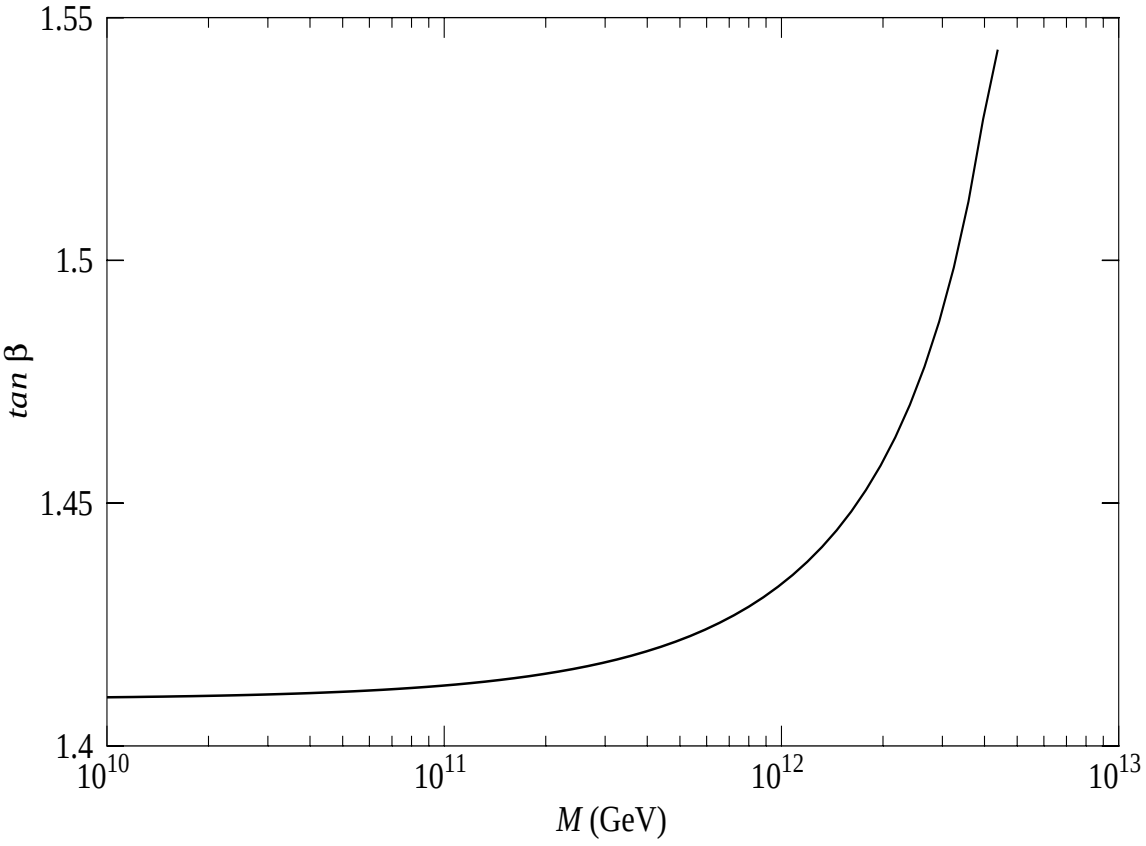

Figure 12: Dependence of lowest value of $\tan\beta$ with the Majorana mass for $m_\nu = 2$ eV.

instance, supposing that the scale at which the effective mass operator is generated is $\Lambda = 10^{11}$ GeV, it can be seen from that figure that an upper limit $\tan\beta \lesssim 7$ is obtained. This was fully confirmed by the see-saw analysis performed in section 3. As discussed in section 2, these upper bounds become weaker as the neutrino mass, m_ν, decreases.

Now, from completely different reasons, neutrino-induced radiative corrections modify the *lower* bound on $\tan\beta$. In the ordinary MSSM the lowest possible value for $\tan\beta$ is derived from the value of the top Yukawa coupling in the infrared fixed point (IFP) limit, by the condition of a physical top mass in agreement with the experiment. In the MSSM extended with right-handed neutrinos, the RGE for Y_t becomes modified in the form

$$\frac{d\mathbf{Y_U}}{dt} = -\frac{\mathbf{Y_U}}{16\pi^2}\left[\left(\frac{13}{15}g_1^2 + 3g_2^2 + \frac{16}{3}g_3^2 - T_2\right)\mathbf{I}_3 - 3\mathbf{Y_U^\dagger Y_U} - \mathbf{Y_D^\dagger Y_D}\right], \qquad (45)$$

(we write the RGE for the full matrix of up-quark Yukawa couplings). If the neutrino Yukawa couplings, $\mathbf{Y}_\nu$, are sizeable (which occurs for large enough m_ν or M), their

contribution tends to lower the value of Y_t further. In consequence, $Y_t(m_{top})$ decreases and the corresponding $\tan\beta$ increases. Fig. 12 shows the new lower bound on $\tan\beta$ for the typical case $m_\nu = 2$ eV. Again, a diagonal structure for the neutrino Yukawa matrix, $\mathbf{Y}_\nu = Y_\nu \mathbf{I_3}$, has been assumed for simplicity. It is important to realize that we cannot raise the value of Y_ν arbitrarily, since then Y_ν develops a Landau pole below M_p, as has been discussed in the previous subsection. This is the reason why the curve shown stops abruptly. As can be seen from the figure (evaluated at the 1-loop level), the change on $\tan\beta$ is very modest, but it may give rise to an increment on the Higgs mass of about 3 GeV, which should be taken into account for precision calculations.

From a more qualitative point of view, we would like to mention two important implications of the presence of massive neutrinos for the supersymmetric perturbative unification.

First, supersymmetric gauge coupling unification is considered as a brilliant success of the MSSM, since the two-loop running of the $SU(3)\times SU(2)\times U(1)$ gauge couplings unifies with great precision at $M_{GUT} \sim 2\times 10^{16}$ GeV. The unification, although remarkable, is not perfect. It is usual to invoke unknown (GUT or superstring) threshold effects in order to explain the discrepance. Since neutrino Yukawa couplings, $\mathbf{Y}_\nu$, give a 2-loop contribution to the g_1 and g_2 gauge couplings (see e.g. [19]), for large enough $\mathbf{Y}_\nu$ (which means large m_ν and/or M) this may be useful for a complete satisfactory unification.

Second, the $\mathbf{Y}_\nu$ couplings have a 1-loop contribution to the charged *lepton* Yukawa couplings, $\mathbf{Y_e}$, see eq.(26). Again, for large $\mathbf{Y}_\nu$, this produces significant variations for $\mathbf{Y_e}$ at low energy, affecting the perturbative bottom-tau unification. This subject has been already addressed in the literature [20]. Due to the form of eq.(26), working in the flavour basis for the charged leptons, the mass eigenvalues m_{e_i} receive a correction from $\mathbf{Y}_\nu$ that, at first order, goes like $\Delta_\nu m_{e_i}^2 \sim R\ m_{e_i}^2 [\mathbf{Y}_\nu^\dagger \mathbf{Y}_\nu]_{ii}$, where R is negative and flavour-independent. Thus, at this order, the neutrino contribution to the m_b/m_τ ratio goes always in the same sense for any $\mathbf{Y}_\nu$ texture. For the (problematic) first two families this means in particular that neutrinos are not useful to rescue the analogous second generation (m_s/m_μ) ratio, since the correction goes in the wrong direction, but they might be useful for the m_d/m_e ratio. In any case, non-trivial $\mathbf{Y}_\nu$ textures will have a significant impact on the supersymmetric m_b/m_τ unification scenarios.

6 Conclusions

We have studied the possibility that neutrinos masses have $\mathcal{O}(eV)$, in order to be cosmologically relevant. In that case they must be nearly degenerate, as required by the oscillation interpretation of atmospheric and solar data. An important question is whether radiative corrections have the right size to account for the small mass splittings required or are generically too large for the scenario to be considered natural. We addressed this problem in the context of the SM (plus three right-handed neutrinos) in a previous publication [9] and, in this paper, we have extended this thorough analysis to the supersymmetric case.

The size of the mass splittings that we find is always much larger than required by the vacuum oscillation solution to the solar neutrino problem, solution which is therefore excluded in this scenario.

When the origin of the non-zero neutrino masses is the see-saw mechanism (we concentrate our study in this appealing case) we find non-negligible regions in parameter space where the mass splittings are consistent with the large angle MSW solution, providing a natural origin for the $\Delta m^2_{sol} \ll \Delta m^2_{atm}$ hierarchy. These regions correspond to Majorana masses around 10^{10} GeV and small $\tan\beta \sim 2$. Concerning the mixing angles, they are remarkably stable and close to the bimaximal mixing form (something that is not guaranteed a priory, due to an ambiguity in the diagonalization of the initial matrix).

We have understood analytically the origin of these remarkable features, giving explicit expressions for the mass splittings and the mixing angles. In particular, we give simple analytical relations between the mixing angles, which are also valid for any model starting with a bimaximal mixing form for the neutrinos. In addition, we have presented particularly simple see-saw ansätze consistent with all atmospheric and solar neutrino observations.

Let us remark that the viability of the scenario is very sensitive to a possible upper bound on $\sin^2 2\theta_3$ (the angle responsible for the solar neutrino oscillations). An upper bound such as $\sin^2 2\theta_3 < 0.99$ would disallow completely the scenario of nearly degenerate neutrinos due to the incompatibility between acceptable mixing angles to fit simultaneously all the neutrino oscillation data. This incompatibility is also easily understood from the analytical relations between the mixing angles, and thus is applies

also for the SM case and more generic models.

Finally we have described in some detail several implications of the existence of (possibly large) neutrino Yukawa couplings. This includes the effects on: the triviality limits on the see-saw Majorana mass, the infrared fixed-point of the top yukawa coupling, and the gauge and bottom-tau unification.

Acknowledgements

This research was supported in part by the CICYT (contract AEN95-0195) and the European Union (contract CHRX-CT92-0004) (JAC). A.I. and I.N. thank the CERN Theory Division for hospitality.

References

[1] Y. Fukuda et al., Super-Kamiokande Collaboration, *Phys. Lett.* **B433** (1998) 9; *Phys. Rev. Lett.* **81** (1998) 1562; S. Hatakeyama et al., Kamiokande Collaboration, *Phys. Rev. Lett.* **81** (1998) 2016; M. Ambrosio et al., MACRO Collaboration, *Phys. Lett.* **B434** (1998) 451.

[2] H. Georgi and S.L. Glashow, [hep-ph/9808293].

[3] F. Vissani, [hep-ph/9708483]; V. Barger, S. Pakvasa, T.J. Weiler and K. Whisnant, *Phys. Lett.* **B437** (1998) 107.

[4] C. Giunti, *Phys. Rev.* **D59**:077301 (1999).

[5] C.D. Carone and M. Sher, *Phys. Lett.* **B420** (1998) 83; A.S. Joshipura, *Z. Phys.* **C64** (1994) 31; A. Ioannisian and J.W.F. Valle, *Phys. Lett.* **B332** (1994) 93; D. Caldwell and R.N. Mohapatra, *Phys. Rev.* **D48** (1993) 3259; G.K. Leontaris, S. Lola, C. Scheich and J.D. Vergados, *Phys. Rev.* **D53** (1996) 6381; S. Lola and J.D. Vergados, *Prog. Part. Nucl. Phys.* **40** (98) 71; B.C. Allanach, [hep-ph/9806294]; A.J. Baltz, A.S. Goldhaber and M. Goldhaber, *Phys. Rev. Lett.* **81** (1998) 5730; R.N. Mohapatra and S. Nussinov, *Phys. Lett.* **B441** (1998) 299 and [hep-ph/9809415]; C. Jarlskog, M. Matsuda and S. Skadhauge, [hep-ph/9812282]; Y. Nomura and T. Yanagida, *Phys. Rev.* **D59**:017303 (1999); S.K. Kang and C.S. Kim, *Phys. Rev.* **D59**:091302 (1999); S. Davidson and S. King,

Phys. Lett. **B445** (1998) 191; H. Fritzsch and Z. Xing, *Phys. Lett.* **B440** (1998) 313 and [hep-ph/9903499]; M. Tanimoto, *Phys. Rev.* **D59**:017304 (1998); N. Haba, *Phys. Rev.* **D59**:035011 (1999); Yue-Liang Wu, [hep-ph/9901245]; E. Ma, [hep-ph/9812344] and [hep-ph/9902465]; E.M. Lipmanov, [hep-ph/9901316]; T. Ohlsson and H. Snellman, [hep-ph/9903252]; A.H. Guth, L. Randall and M. Serna, [hep-ph/9903464]; G.C. Branco, M.N. Rebelo and J.I. Silva-Marcos, *Phys. Rev. Lett* **82** (1999) 683; Y.-L. Wu., [hep-ph/990522].

[6] J. Ellis and S. Lola, [hep-ph/9904279].

[7] C.S. Aulakh and R.N. Mohapatra, *Phys. Lett.* **B119** (1982) 136; *Phys. Lett.* **B121** (1982) 147; L.J. Hall and M. Suzuki, *Nucl. Phys.* **B231** (1984) 419.

[8] C.S. Aulakh, A. Melfo, A. Rašin and G. Senjanović, [hep-ph/9902409].

[9] J.A. Casas, J.R. Espinosa, A. Ibarra and I. Navarro, [hep-ph/9904395].

[10] R. Barbieri et al., *JHEP* **9812** (1998) 017; G.L. Fogli, E. Lisi, A. Marrone and G. Scioscia, *Phys. Rev.* **D59**:033001 (1999), [hep-ph/9904465].

[11] L. Baudis et al., Heidelberg-Moscow exp., [hep-ex/9902014].

[12] V. Lobashev, Pontecorvo Prize lecture at the JINR, Dubna, January 1999; A.I. Belesev et al., *Phys. Lett.* **B350** (1995) 263.

[13] Y. L. Wu, [hep-ph/9810491], [hep-ph/9901245] and [hep-ph/9901320]; C. Wetterich, [hep-ph/9812426]; R. Barbieri, L.J. Hall, G.L. Kane, and G.G. Ross, [hep-ph/9901228]; M. Tanimoto, T. Watari, T. Yanagida, [hep-ph/9904338].

[14] K. Babu, C. N. Leung and J. Pantaleone, *Phys. Lett.* **B319** (1993) 191.

[15] M. Gell-Mann, P. Ramond and R. Slansky, proceedings of the Supergravity Stony Brook Workshop, New York, 1979, eds. P. Van Nieuwenhuizen and D. Freedman (North-Holland, Amsterdam); T. Yanagida, proceedings of the Workshop on Unified Theories and Baryon Number in the Universe, Tsukuba, Japan 1979 (edited by A. Sawada and A. Sugamoto, KEK Report No. 79-18, Tsukuba); R. Mohapatra and G. Senjanović, *Phys. Rev. Lett.* **44** (1980) 912, *Phys. Rev.* **D23** (1981) 165.

[16] N. Haba, N. Okamura and M. Sugiura, [hep-ph/9810471], [hep-ph/9904292]

[17] J.A. Casas, V. Di Clemente, A. Ibarra and M. Quirós, [hep-ph/9904295].

[18] A. De Rújula, M.B.Gavela and P. Hernández, [hep-ph/9811390].

[19] Yu.F. Pirogov, O. V. Zenin, [hep-ph/9808396].

[20] F. Vissani and A. Yu. Smirnov, *Phys. Lett.* **B341** (1994) 173; A. Brignole, H. Murayama and R. Rattazzi, *Phys. Lett.* **B335** (1994) 345; G. K. Leontaris, S. Lola, G. G. Ross, *Nucl. Phys.* **B454** (1995) 25; M. Bando and K. Yoshioka, *Phys. Lett.* **B444** (1998) 373.